Scientia Iranica B (2014) 21(5), 1683–1692

Sharif University of Technology
Scientia Iranica
Transactions B: Mechanical Engineering
www.scientiairanica.com

Normalized miss distance analysis of single-lag optimal guidance law with radome effect, saturation and fifth-order control system

S.H. Jalali-Naini*

Faculty of Mechanical Engineering, Tarbiat Modares University, Tehran, P.O. Box 14115-111, Iran.

Received 1 November 2012; received in revised form 12 August 2013; accepted 30 December 2013

KEYWORDS
Miss distance;
Radome effect;
First-order optimal guidance;
Proportional navigation.

Abstract. This paper deals with miss distance analysis of single-lag Optimal Guidance Law (OGL) using linearized equations of motion in normalized form. The radome refraction error, acceleration limit, constant target acceleration, and arbitrary-order binomial guidance and control system are considered in the formulation. In addition, body rate feedback is utilized in the OGL formulation as a well-known classical compensation method of radome effect for proportional navigation guidance. The numerical solution of normalized equations produces normalized miss distance curves, which are useful tools for guidance designer for analysis and design of guidance parameters for an allowable miss distance and acceleration limit. Moreover, a modified first-order guidance scheme, based on an analytical stability analysis and normalized miss distance curves, is presented for reducing the achievable miss distance.

1. Introduction

The radome refraction effect has an important role in the stability and miss distance of radar homing interceptors. The radome refraction of incoming electromagnetic wave creates an unwanted feedback path in the homing guidance loop, which causes false interceptor-to-target Line-Of-Sight (LOS) due to the interceptor turning rate [1-3]. A thorough explanation of radome effect has been presented in [4]. Proportional Navigation (PN) and its variants use LOS rate for calculating the acceleration command. This class of guidance laws has been widely used for its simplicity and ease of implementation [5].

One of the most powerful methods for miss distance analysis is the adjoint method. The adjoint method can produce the miss distance by a single run of the numerical solution for all possible flight times. The adjoint method does not work for nonlinear guidance laws or when interceptor acceleration limit is imposed. The covariance analysis and Monte Carlo methods can also be used for miss distance analysis. The covariance analysis, similar to the adjoint method, is restricted to linear systems [5]. Another method of miss distance analysis uses normalized governing equations to produce miss distance curves for homing loop analysis and design. The method can generate normalized design curves for all possible flight times, interceptor-to-target acceleration ratio, guidance and control time constant, and other parameters. The normalized PN miss distance curves can be found in Ref. [5] for the first-order guidance and control system without acceleration saturation and radome effects, and for the fifth-order system with saturation and no radome effect. Neslin and Zarchan [6] presents several normalized miss distance curves versus dimensional parameters for PN. Approximate normalized miss distance curves due to seeker noises are available in Ref. [7] for PN in the presence of radome effect

*. *Tel.: +98 21 82883936; Fax: +98 21 82884909*
E-mail address: shjalalinaini@modares.ac.ir

and no acceleration limit. Moreover, extensive works have been done for radome effect on PN homing loop without normalization. However, results of these studies depend on the individual values of the studied parameters [8-10]. In Ref. [11] the normalized analysis of miss distance was presented for PN with saturation, radome effect, and body rate feedback for the first-order guidance and control system. It was also shown that the normalized analysis could be applied to some nonlinear types of guidance laws [11].

Most of the literature on the radome refraction effect deals with the miss distance analysis of PN guidance law and its compensation. Optimal Guidance Laws (OGLs) have been developed to account for the interceptor guidance and control dynamics, which can be modeled by first, second, or higher-order transfer functions. The first-order (single-lag) OGL, derived in Ref. [12], has been compared in Ref. [13] with PN in terms of performance and sensitivity to errors, such as radome error slope, considering a first-order control system using dimensional curves of miss distance which produces case dependent results. However, since the single-lag OGL is obtained assuming a first-order control system, the miss distance analysis should be carried out for the higher-order control system; otherwise the comparison will not be justified. In addition, the radome-induced miss distance curves in Ref. [13] do not consider the acceleration saturation.

More advanced guidance laws are the second-order OGL [14] and high-order OGL [15], which account for the second- and high-order guidance and control dynamics, respectively. The first-order OGL is utilized for minimum phase guidance and control system with equivalent time constant, e.g. canard control interceptors. The higher order guidance laws have mainly been developed for nonminimum phase interceptors [15]. The OGLs may also be modified by the introduction of a time-weighted performance index [16], or shaping the commanded acceleration for minimum and nonminimum phase control systems [17]. These references have compared the performance of OGLs and its modified versions with PN and simplified OGLs, without considering the radome effect. Few works in the open literature have analyzed the radome effect on the performance of advanced guidance laws. An integrated guidance and control scheme has been developed in Ref. [18], which considers the radome effect, without including the simulation results. The high-order guidance laws need estimation of more quantities and their performance degrades in the presence of noise and unmodeled dynamics. The other type of modification of PN is pseudoclassical guidance law in which its commanded acceleration is calculated by two terms; the first term being similar to True PN (TPN), and the second term consisting of the difference between the TPN commanded acceleration and the achieved commanded acceleration passing through an appropriate transfer function, such as a lead-lag compensator or a PD/PID [19]. The pseudoclassical guidance scheme has similarities in structure with the first-order OGL for the case of constant gains.

There are classical and modern methods for compensation of radome refraction. The body rate feedback is one of the classical methods used for this purpose [20]. The lead-lag networks are utilized through this feedback path to improve the frequency response of the guidance and control system. There are numerous methods, based on modern estimation and filtering theory, which are beyond the scope of this work; for example, radome slope compensation using multiple-model Kalman filters [21], adaptive particle filter [22], neural network [23], interacting multiple model algorithm [24], in-flight two-step nonlinear estimation of radome aberration [25], and slope estimation in flight using fuzzy adaptive multiple model [26]. A different method is the estimation of radome slope from information generated by dither and extracted by bandpass filtering [27,28].

This work presents the miss distance analysis of single-lag optimal guidance law using normalized governing equations taking into account the acceleration saturation and radome effect for the fifth-order binomial guidance and control system. Moreover, the formulations and obtained results lead to some modifications of this type of guidance law. The method can also be applied to a wide-variety of guidance schemes such as pseudoclassical guidance law.

2. Linearized equations

The linearized equation of motion, as the one-dimensional case, is written as follows [5]:

$$\ddot{y} = n_T - n_M, \tag{1}$$

where y is the separation between interceptor M and target T along axis 2, n_M is the interceptor acceleration, and n_T is the target acceleration as shown in Figure 1. The subscripts M and T denote interceptor

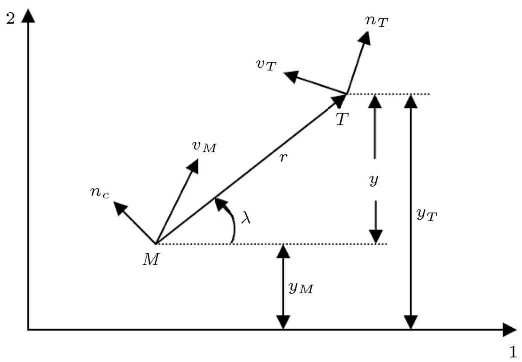

Figure 1. Engagement geometry.

and target, respectively. Also, v stands for velocity and r is the distance between the interceptor and its target. Axis 1 is defined as a line through the initial positions of the interceptor and its targets, and axis 2 is perpendicular to this axis. Using small angle approximation, the LOS angle is given by $\lambda = y/r$ (see Figure 1). Therefore, the LOS rate is found to be [5]:

$$\dot{\lambda} = \frac{y + \nu t_{\mathrm{go}}}{v_c t_{\mathrm{go}}^2}. \tag{2}$$

Here $\nu = \dot{y}$, and v_c is the closing velocity assumed to be constant for the problem which leads to the linearized range equation, i.e. $r = v_c t_{\mathrm{go}}$, where $t_{\mathrm{go}} = t_f - t$ is the time-to-go until intercept, t is the current time, and t_f is the intercept time.

The commanded acceleration for a class of guidance laws can be expressed as follows:

$$n_c = N' v_c(\dot{\lambda}_m + K_B\dot{\theta}) - N'_L n_L, \tag{3}$$

where N' and N'_L are navigation coefficients; θ and λ_m are the angles of the interceptor longitudinal axis and LOS with respect to axis 1, respectively; K_B is the gain of body rate feedback; and n_L is the lateral acceleration, which equals n_M for the linearized problem.

The radome refraction angle r_{dome} is assumed to be linearly proportional to the interceptor look angle [5], that is:

$$r_{\mathrm{dome}} = R(\lambda - \theta), \tag{4}$$

where R is a constant known as the radome slope.

As shown in Figure 2, the measured LOS angle (λ_m) in terms of the radome slope is given by:

$$\lambda_m = \lambda + r_{\mathrm{dome}} = (1+R)\lambda - R\theta. \tag{5}$$

Taking time derivative of Eq. (5) yields:

$$\dot{\lambda}_m = \dot{\lambda} + \dot{r}_{\mathrm{dome}} = (1+R)\dot{\lambda} - R\dot{\theta}. \tag{6}$$

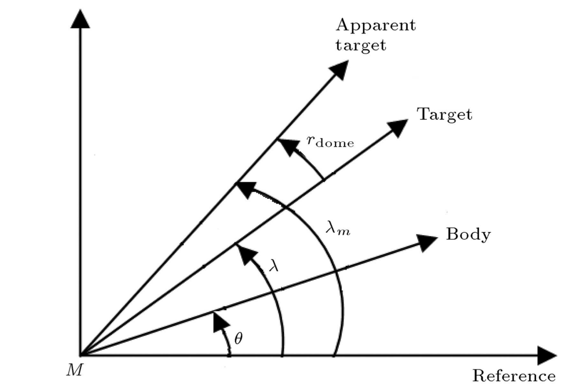

Figure 2. Basic geometry for radome analysis.

Substitution of Eq. (6) in Eq. (3) gives the commanded acceleration in terms of the true LOS rate:

$$n_c = N' v_c\left[(1+R)\dot{\lambda} - (R - K_B)\dot{\theta}\right] - N'_L n_L. \tag{7}$$

The interceptor body rate can be written in terms of the turning rate time constant (T_α = angle of attack/$\dot{\gamma}$), interceptor speed, and lateral acceleration, $n_L = v_M\dot{\gamma}$, where γ is the interceptor flight path angle, that is [5]:

$$\dot{\theta} = \frac{n_L}{v_M} + \frac{T_\alpha}{v_M}\dot{n}_L. \tag{8}$$

When the interceptor acceleration limit, A_{sat}, is considered in the modeling, the commanded acceleration is denoted by a_c, whereas n_c stands for the saturated commanded acceleration; therefore:

$$n_c = \begin{cases} A_{\mathrm{sat}}\ \mathrm{sgn}(a_c) & |a_c| > A_{\mathrm{sat}} \\ a_c & |a_c| \le A_{\mathrm{sat}} \end{cases} \tag{9}$$

In the case of the first-order guidance and control system with time constant T, we have:

$$\dot{n}_L = (n_c - n_L)/T \tag{10}$$

or:

$$\frac{n_L}{n_c} = \frac{1}{1+Ts}, \tag{11}$$

where s is the Laplace domain variable. In the presence of radome effect, the single-lag OGL becomes unstable even for the first-order model of guidance and control system. In this case, acceleration command (7) can be rewritten in terms of n_L for the case of no acceleration limit ($n_c = a_c$) to show the instability problem when the denominator in the following equation goes to zero, that is:

$$n_c = \frac{N' v_c(1+R)\dot{\lambda} - K_{eq}\left(1 - \frac{T_\alpha}{T}\right)n_L - N'_L n_L}{1 + K_{eq}(T_\alpha/T)}, \tag{12}$$

where:

$$K_{eq} = \frac{N' v_c(R - K_B)}{v_M}. \tag{13}$$

Also, the equivalent radome slope can be defined by $R_{eq} = R - K_B$. The navigation coefficients for the single-lag OGL are given by [12]:

$$N'_{\mathrm{OPT}} = \frac{6z^2(e^{-z} - 1 + z)}{2z^3 + 3 + 6z - 6z^2 - 12ze^{-z} - 3e^{-2z}}, \tag{14}$$

$$K_L = \frac{e^{-z} - 1 + z}{z^2}, \qquad N'_L = N'_{\mathrm{OPT}} K_L, \tag{15}$$

where $z = t_{go}/T$. Also, K_L varies from relatively small values at the beginning of the engagement (depending on how large $z = t_{go}/T$ is) and approaches 0.5 as z goes to zero, i.e. at intercept time.

The n-order binomial model of the guidance and control system is given by [5]:

$$\frac{n_L}{n_c} = 1/\left(1 + \frac{T}{n}s\right)^n. \tag{16}$$

The state space representation of the preceding transfer function may be obtained by breaking the n-order transfer function into a series of multiplying single-lag blocks, that is:

$$\begin{cases} T_n\dot{x}_3 = -x_3 + n_c \\ T_n\dot{x}_4 = -x_4 + x_3 \\ \vdots \\ T_n\dot{x}_{n+2} = -x_{n+2} + x_{n+1} \end{cases} \tag{17}$$

where $T_n = T/n$ and $x_{n+2} = n_L$ $(n > 1)$. The state variable $x_j (j = 3, \cdots, n+2)$ begins with $j = 3$, because the first two state variables are $x_1 = y$ and $x_2 = \nu$.

3. Stability analysis

Here, the stability analysis of guidance Eq. (7) is carried out without the saturation effect. The transfer function from LOS rate to interceptor acceleration can be found using Eqs. (7), (8) and (16) as follows:

$$\frac{n_L}{\dot{\lambda}} = \frac{N' v_c(1+R)}{\left(1+\frac{T}{n}s\right)^n + K_{eq}(1+T_\alpha s) + N'_L}. \tag{18}$$

The effective value for navigation ratio is the DC gain of the preceding transfer function divided by closing velocity, that is:

$$N'_{\text{Eff}} = \frac{N'(1+R)}{1+K_{eq}+N'_L} > 0. \tag{19}$$

It follows that the radome slope, body rate feedback, and N'_L influence the effective value of the navigation ratio. As known from the LOS rate behavior of TPN, N'_{Eff} must be greater than 2 in order to prevent guidance instability [29].

For the first-order guidance and control system $(n = 1)$ we have:

$$\frac{n_L}{\dot{\lambda}} = \frac{N'_{\text{Eff}} v_c}{1 + T_{\text{Eff}} s}, \tag{20}$$

where:

$$T_{\text{Eff}} = \frac{T\left(1 + \frac{T_\alpha}{T}K_{eq}\right)}{1+K_{eq}+N'_L} > 0. \tag{21}$$

For the second-order guidance and control system $(n = 2)$ we have:

$$\frac{n_L}{\dot{\lambda}} = \frac{N'_{\text{Eff}} v_c}{1 + \frac{2\xi}{\omega_n}s + \frac{1}{\omega_n^2}s^2}, \tag{22}$$

where:

$$\xi = \frac{1 + \frac{T_\alpha}{T}K_{eq}}{\sqrt{1+K_{eq}+N'_L}}, \tag{23}$$

$$\omega_n = \frac{2\sqrt{1+K_{eq}+N'_L}}{T}. \tag{24}$$

For brevity we define:

$$c = 1 + K_{eq} + N'_L, \tag{25}$$

$$X = 1 + \frac{T_\alpha}{T}K_{eq}. \tag{26}$$

Therefore, the stability criteria for the second-order guidance and control system $(n = 2)$ can be simply written as:

$$c > 0 \quad \text{and} \quad X > 0. \tag{27}$$

The stability criteria for the third-order guidance and control system $(n = 3)$ are also obtained as:

$$c > 0 \quad \text{and} \quad X > c/9. \tag{28}$$

The stability criteria for the fourth-order guidance and control system $(n = 4)$ are obtained as follows:

$$\begin{cases} 0 < c < 9 \\ 3 - \sqrt{9-c} < X < 3 + \sqrt{9-c} \end{cases} \tag{29}$$

The guidance and control characteristic equation for $n = 5$ becomes:

$$\mu^5 + 5\mu^4 + 10\mu^3 + 10\mu^2 + 5\mu X + c = 0, \tag{30}$$

where $\mu = Ts/5$. To better trace the derivations, the notations used are similar to Ref. [7]. The coefficients of the characteristic equation are denoted by:

$$\begin{cases} B_5 = 1,\ B_4 = 5,\ B_3 = 10 \\ B_2 = 10,\ B_1 = 5X,\ B_0 = c \end{cases} \tag{31}$$

According to the Routh criterion, the guidance and control transfer function is stable if coefficients $B_0, \cdots, B_5$ and the following quantities are all positive:

$$a_1 = \frac{B_4 B_3 - B_5 B_2}{B_4}, \tag{32a}$$

$$b_1 = \frac{a_1 B_2 - B_4 a_2}{a_1}, \tag{32b}$$

$$c_1 = \frac{b_1 a_2 - a_1 b_2}{b_1}, \tag{32c}$$

$$d_1 = b_2 = c, \tag{32d}$$

where:

$$a_2 = \frac{B_4 B_1 - B_5 B_0}{B_4}. \tag{33}$$

After some manipulation, the stability criteria lead to:

$$\begin{cases} c > 0 \quad \text{and} \quad X > 0 \\ b_1 = 10 - \frac{25}{8}X + \frac{c}{8} > 0 \\ c_1 b_1 = \left(10 - \frac{25}{8}X + \frac{c}{8}\right)\left(5X - \frac{c}{5}\right) - 8c > 0 \end{cases} \tag{34}$$

The last two inequalities in Relation (34) are simplified to:

$$X < \frac{55 + c}{25}, \tag{35}$$

$$25X^2 - 2(40 - c)X + 16c + \frac{c^2}{25} < 0. \tag{36}$$

To satisfy Inequality (36), X must lie between the two roots of the left-hand side of the inequality, provided that $c < 5$, that is, $X_1 < X < X_2$ where:

$$X_1 = \frac{8}{5} + \frac{c}{25} - \frac{8}{5}\sqrt{1 - \frac{c}{5}}, \tag{37a}$$

$$X_2 = \frac{8}{5} + \frac{c}{25} + \frac{8}{5}\sqrt{1 - \frac{c}{5}}. \tag{37b}$$

Hence, using all the obtained inequalities, the stability criteria for the fifth-order binomial guidance and control system become:

$$0 < c < 5 \quad \text{and} \quad X_1 < X < X_2. \tag{38}$$

It should be noted that the coefficient c is itself a function of K_{eq}. Stable and unstable regions are illustrated in Figure 3 for the third- to fifth-order guidance and control systems. For $n = 1, 2$, the complete first quadrant, excluding the axes, is the stable region. For $n = 3$, the region above the dash-dotted line ($X = c/9$) in the first quadrant is stable. For $n = 4$ and 5, upper bounds for c and X appear, contrary to the case of $n = 1, 2, 3$. The regions inside the solid line and dotted line in the first quadrant are stable regions for $n = 4$ and 5, respectively.

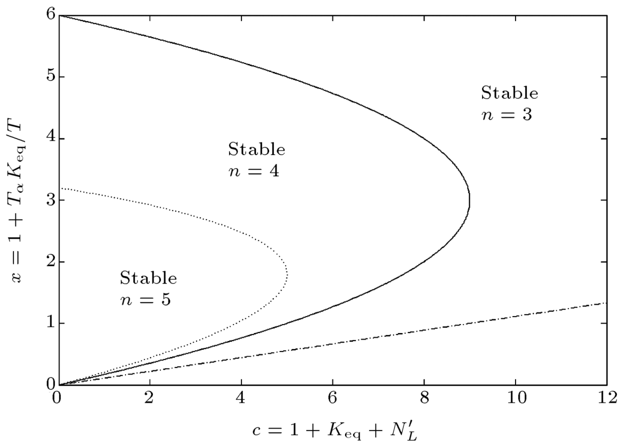

Figure 3. Stable regions for $n = 3, 4, 5$.

The stability regions may be displayed using axis T_α/T versus axis c (or $K_{eq} + N'_L$). Also, approximate criteria may be obtained for the stability regions. For example, for $c = 1$, we have:

$$-0.791 < \frac{T_\alpha}{T} K_{eq} < 2.071. \tag{39}$$

In the case of $N'_L = 0$, the preceding inequality may be considered as an approximate criterion for the stability of the fifth-order binomial guidance and control system as treated in Ref. [7], provided that $-1 < K_{eq} < 4$. In this case, the stable region lies between the two curves, $T_\alpha/T = (-1 + X_{1,2}(K_{eq}))/K_{eq}$, for a specified value of N'_L.

4. Normalized equations

The system equations can be normalized using the following change of variables:

$$\tau = \frac{t}{T}, \qquad \tau_f = \frac{t_f}{T}, \tag{40a}$$

$$\hat{y} = \frac{y}{|n_T| T^2}, \qquad \hat{\nu} = \frac{\nu}{|n_T| T}, \tag{40b}$$

$$\hat{n}_L = n_L/|n_T|, \qquad \hat{n}_c = n_c/|n_T|, \tag{40c}$$

$$\hat{\theta} = \frac{v_M \theta}{T|n_T|}, \qquad \hat{\lambda} = \frac{v_c \lambda}{T|n_T|}. \tag{40d}$$

As we consider only a maneuvering target with constant acceleration, the initial heading error is assumed to be zero. The initial value for $\hat{y}$ is zero because of the definition of axis 1 in Figure 1. Since, the initial heading error is assumed to be zero, $\hat{\nu}$ is set to zero at $t = 0$.

The normalized form of Eqs. (2) and (8) are given by:

$$\hat{\lambda}' = \frac{\hat{y} + \hat{\nu} z}{z^2}, \tag{41}$$

$$\hat{\theta}' = \hat{n}_L + \frac{T_\alpha}{T}\hat{n}'_L, \tag{42}$$

where $()'$ stands for $d()/d\tau$. Also, the acceleration command and its saturated form can be normalized as follows:

$$\hat{a}_c = N'(z)(1 + R)\hat{\lambda}' - K_{\text{eq}}(z)\hat{\theta}' - N'_L(z)\hat{n}_L, \tag{43}$$

$$\hat{n}_c = \begin{cases} R_{\text{sat}} \ \text{sgn}(\hat{a}_c) & |\hat{a}_c| > R_{\text{sat}} \\ \hat{a}_c & |\hat{a}_c| \le R_{\text{sat}} \end{cases} \tag{44}$$

where $\hat{a}_c = a_c/|n_T|$ and $R_{\text{sat}} = A_{\text{sat}}/|n_T|$.

4.1. First-order G&C system

The normalized equations for the first-order guidance and control system ($n = 1$) are obtained as follows:

$$\begin{cases} \hat{y}' = \hat{\nu} \\ \hat{\nu}' = \text{sgn}(n_T) - \hat{n}_L \\ \hat{n}_L' = \hat{n}_c - \hat{n}_L \end{cases} \tag{45}$$

where $\hat{a}_c$ and $\hat{n}_c$ are calculated from Eqs. (43) and (44). By substituting Eq. (42) and the last term in Eq. (45) into Eq. (43), $\hat{a}_c$ can be rewritten for the case of no acceleration limit ($\hat{n}_c = \hat{a}_c$) as follows:

$$\hat{a}_c = \frac{N'(z)(1+R)\hat{\lambda}' - K_{\text{eq}}(z)\left(1-\frac{T_\alpha}{T}\right)\hat{n}_L - N_L'(z)\hat{n}_L}{1 + K_{\text{eq}}(z)\frac{T_\alpha}{T}}. \tag{46}$$

4.2. The nth-order binomial G&C system

The normalized equations for the nth-order binomial model of the guidance and control system are obtained in the following form:

$$\begin{cases} \hat{y}' = \hat{\nu} \\ \hat{\nu}' = \text{sgn}(n_T) - \hat{n}_L \\ \hat{x}_3' = n\left(-\hat{x}_3 + \hat{n}_c\right) \\ \hat{x}_4' = n\left(-\hat{x}_4 + \hat{x}_3\right) \\ \vdots \\ \hat{x}_{n+2}' = n\left(-\hat{x}_{n+2} + \hat{x}_{n+1}\right) \end{cases} \tag{47}$$

where $\hat{x} = x/|n_T|$ and $\hat{x}_{n+2} = \hat{n}_L$ ($n > 1$). Substituting Eq. (42) in Eq. (43) yields:

$$\hat{a}_c = N'(1+R)\hat{\lambda}' - \left(N_L' + K_{\text{eq}} - nK_{\text{eq}}\frac{T_\alpha}{T}\right)\hat{n}_L - nK_{\text{eq}}\frac{T_\alpha}{T}\widehat{x}_{n+1}. \tag{48}$$

Also, $\hat{\lambda}'$ and $\hat{n}_c$ are calculated from Eqs. (41) and (44), respectively. It should be noted that Eq. (42) may be added to the state equations, if we need the values of $\hat{\theta}$. The miss distance, MD, is approximated by $|y(t_f)|$, obtained by numerical solution of the linearized equations. Here, the normalized miss distance, $\widehat{\text{MD}} = \text{MD}/(|n_T|T^2)$, is determined using the numerical solution of the normalized equations when the initial conditions for all the state variables are set to zero.

5. Modified first-order guidance law

The single-lag OGL generates smaller miss distance than that of PN when total flight time is relatively small [5], as seen in Figure 4(a). An observation of Figure 4(a) may imply that if PN is initially used, followed by the OGL at the end of engagement, the resulted miss distance for all the total flight times will be modified such that the miss distance will be similar to that of OGL and PN for small flight times and the remaining total fight times, respectively. However, the numerical solution does not show such behavior. The normalized miss distance of OGL, obtained for the fifth-order binomial guidance and control ($n = 5$) without radome effect ($K_{eq} = 0$), versus t_f/T, is illustrated in Figure 4(a) and (b) by solid line, PN (with $N' = 4$) by dotted line marked with plus signs, and PN+OGL given in Eq. (49) by dashed line. As shown in Figure 4(a), the miss distance for Eq. (49) is still inferior compared to that of PN for $t_f > 7.8T$ (with no acceleration limit).

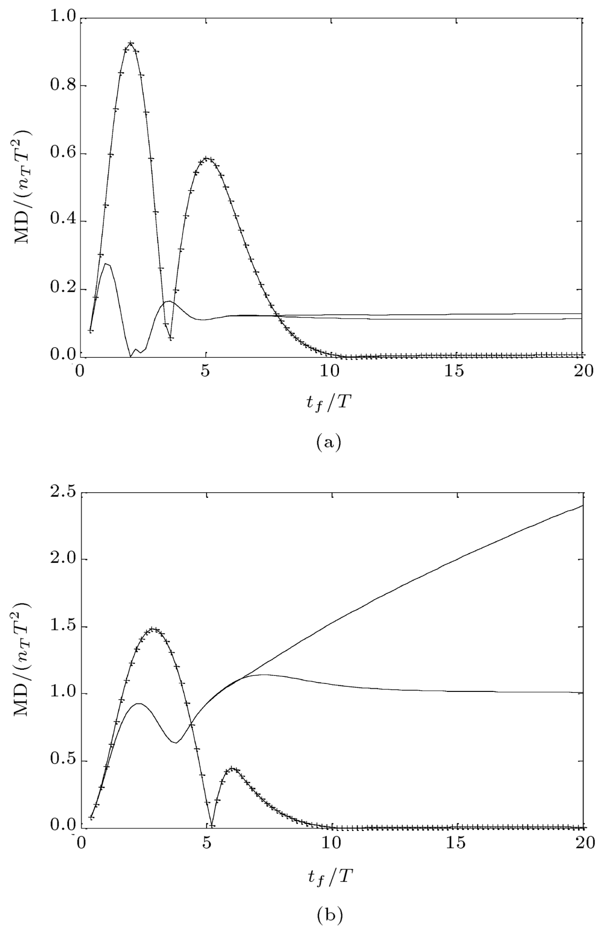

Figure 4. Normalized MD vs normalized flight time without radome effect: a) Without acceleration limit; and b) with acceleration ratio of 3.

$$a_c = \begin{cases} \text{PN}(N' = 4) & \text{for} \quad z > 5 \\ \text{OGL} & \text{for} \quad z \leq 5 \end{cases} \tag{49}$$

The results are obtained for $t_f/T = 0.4$ to 20 with step size of 0.2; the integration step for the normalized time

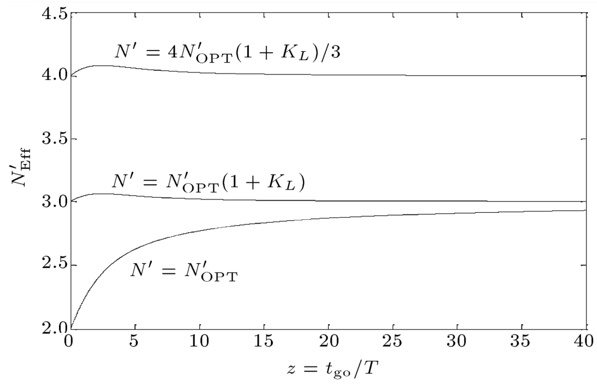

Figure 5. Effective navigation ratio vs normalized time-to-go.

is 0.0002. The miss distance is considerably increased when an acceleration ratio of $R_{\mathrm{sat}} = 3$ is imposed as shown in Figure 4(b). The figure shows that the difference between OGL and OGL+PN increases when an acceleration ratio of 3 is imposed. It should be noted that Eqs. (14) and (15) give optimal gains only for the case of first-order guidance and control system without acceleration limit and radome effect. However, here reference to OGL means referring to Eqs. (14) and (15), which are not optimal gains for the other cases.

The navigation ratio N'_{OPT} has very large values for small values of $z = t_{\mathrm{go}}/T$. Therefore, the effective navigation ratio becomes $1/K_L = 2$ for small values of z as depicted in Figure 5. The navigation ratio may be determined so as to modify the profile of the effective navigation ratio. If the navigation ratio is chosen as $N' = N'_{\mathrm{OPT}}(1 + K_L)$ with the same $N'_L = N'_{\mathrm{OPT}}K_L$, the effective navigation ratio becomes nearly constant and attains the value of 3 as shown in Figure 5. Also, if $N' = 4N'_{\mathrm{OPT}}(1 + K_L)/3$, we have $N'_{\mathrm{Eff}} \approx 4$ for which the resulted miss distance, compared to that of OGL and PN with $N' = 4$, is illustrated in Figure 6(a) using legends similar to Figure 4 ($R_{\mathrm{sat}} = 3$). As expected, the miss distance reduces considerably when the modified navigation ratio is used.

As mentioned earlier, the navigation ratio N'_{OPT} has very large values for small values of $z = t_{\mathrm{go}}/T$. The other modification is to restrict the value of navigation ratio. For example, when $N' = 4(1 + 4K_L)$ and $N'_L = 4K_L$ we have $N'_{\mathrm{Eff}} = 4$. In Figure 6(b), using similar legends as Figure 4, the resultant normalized miss distance is depicted by dashed-line and is compared to that of OGL and PN with $N' = 4$ ($R_{\mathrm{sat}} = 3$).

In the next step, a correction factor and switching parameter, k_c, may be chosen as follows:

$$k_c = \begin{cases} 0 & \text{for} \quad z \geq Z_2 \\ K_f \left(\frac{Z_2 - z}{Z_2 - Z_1}\right)^m & \text{for} \quad Z_1 < z < Z_2 \\ K_f & \text{for} \quad z \leq Z_1 \end{cases} \tag{50}$$

where K_f, Z_1, Z_2 and m are constants. In the guidance law, K_L is replaced by $k_c K_L$. Therefore, the modified single-lag guidance law takes the following form:

$$a_c = 4(1+4k_cK_L)\left[v_c\left(\dot{\lambda}_m + K_B\dot{\theta}\right) - \frac{k_cK_L}{1+4k_cK_L}n_L\right], \tag{51}$$

with $N'_{\mathrm{Eff}} = 4$ regardless of the value of k_c. In Figure 6(c) the normalized miss distance is displayed

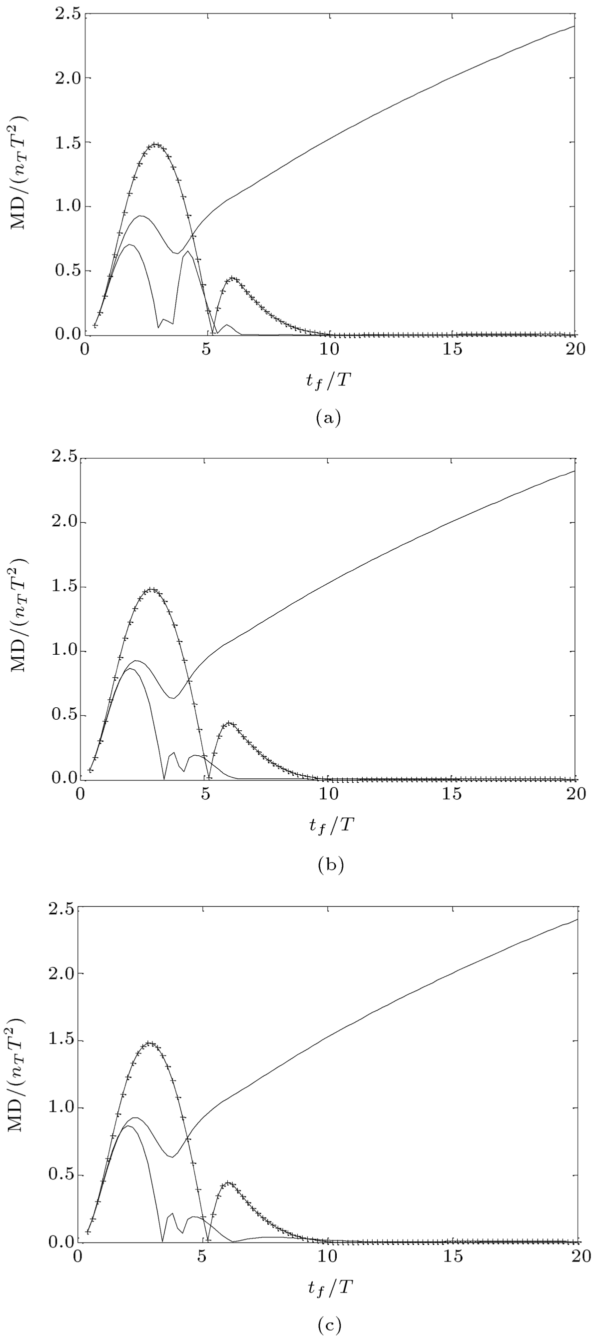

Figure 6. Normalized MD vs normalized flight time with modified navigation coefficients:
a) $N' = 4N'_{\mathrm{OPT}}(1 + K_L)/3$, $N'_L = N'_{\mathrm{OPT}}K_L$; b) $N' = 4(1 + 4K_L)$, $N'_L = 4K_L$; and c) with correction factor (50).

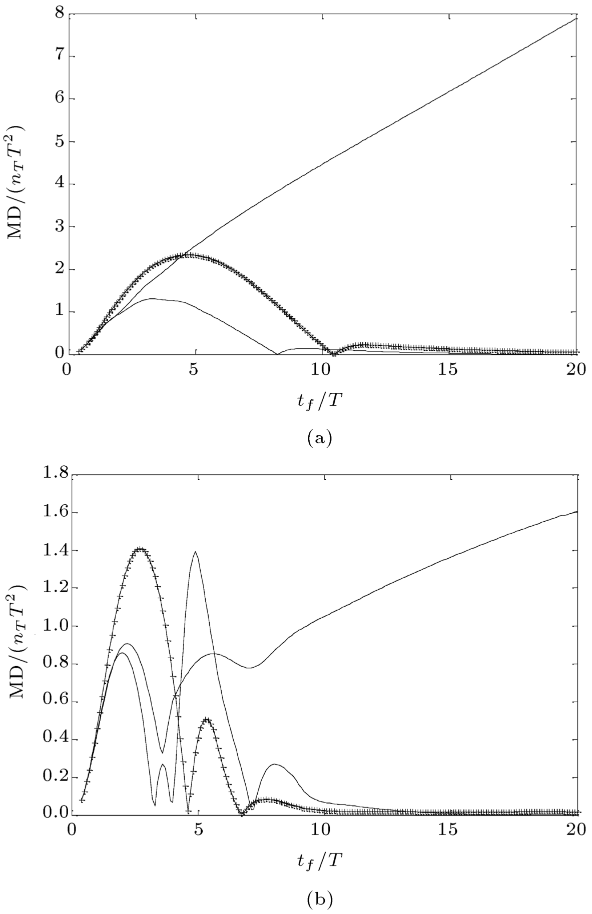

Figure 7. Normalized MD vs normalized flight time with radome effect ($T_\alpha/T = 5$, $R_{\text{sat}} = 3$): a) $v_c R_{eq}/v_M = 0.04$; and b) $v_c R_{eq}/v_M = -0.01$.

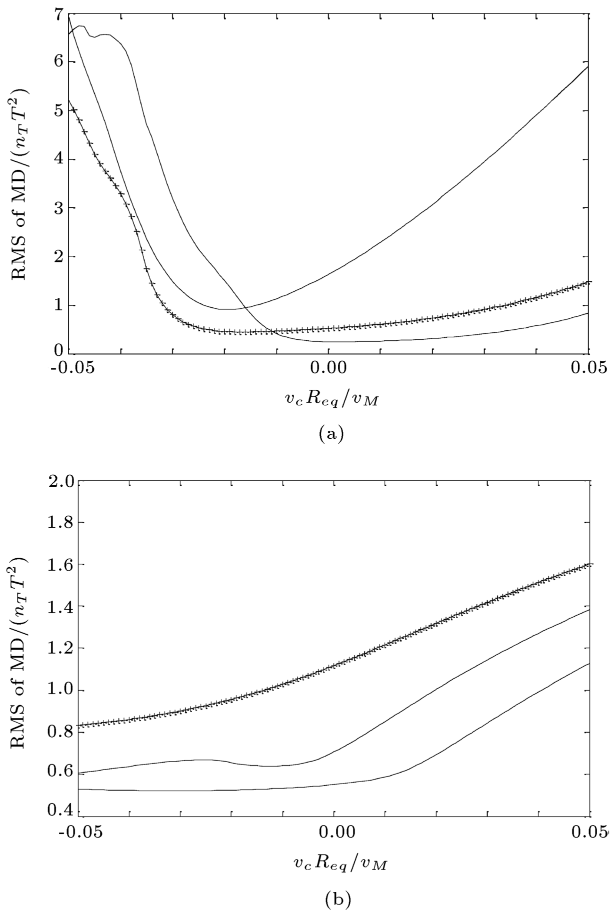

Figure 8. RMS of normalized MD for different intervals of t_f/T with $T_\alpha/T = 5$ and $R_{\text{sat}} = 3$: a) $t_f/T = [0.4\ 20]$; and b) $t_f/T = [0.4\ 4]$.

for $K_f = 1$, $Z_1 = 5$, $Z_2 = 6$, $m = 1$ and $R_{\text{sat}} = 3$, and is compared to that of OGL and PN (with $N' = 4$) as before.

6. Results and discussion

The miss distance of OGL is compared with that of PN and modified first-order guidance (51) in the presence of radome effect for the fifth-order binomial guidance and control system. The achieved commanded acceleration and body turning rate are assumed to be known perfectly.

The normalized miss distance of OGL in Figures 7-9 is illustrated by solid line, PN (with $N' = 4$) by dotted line marked by plus signs, modified first-order guidance given in Eq. (51) by dashed line. Figure 7(a) and (b) depict the normalized miss distance versus normalized flight time for $v_c R_{eq}/v_M = 0.04$ and -0.01, respectively ($T_\alpha/T = 5$, $R_{\text{sat}} = 3$). As shown in Figure 7(a), the miss distance of the modified first-order guidance is less than that of OGL and PN for $v_c R_{eq}/v_M = 0.04$ and $T_\alpha/T = 5$, whereas for negative R_{eq} the results are different; however, the miss distance of the modified first-order guidance is less than that of the two guidance laws for the end game under the mentioned assumptions. The Root Mean Square (RMS) of the normalized miss distance is defined over a discretized interval for normalized intercept time, e.g. $\tau_f = [0.4\ \ 20]$ by step size of 0.2; therefore:

$$\text{RMS}\left(\widehat{\text{MD}}\right) = \left[\frac{1}{S}\sum_{j=1}^{S}\left(\frac{\text{MD}_j}{T^2 n_T}\right)^2\right]^{1/2}, \tag{52}$$

where MD_j is the miss distance at τ_f for the jth step up to the final step S. Using the mentioned definition, the RMS of normalized miss distance can be plotted versus $v_c R_{eq}/v_M$ as shown in Figures 8 and 9 for the three mentioned guidance laws when $R_{\text{sat}} = 3$. The RMS of normalized MD is displayed in Figures 8(a) and 9(a) for $T_\alpha/T = 5$ and 10, respectively, and the mentioned interval for τ_f with the step size of 0.2. Similarly, Figures 8(b) and 9(b) show RMS of normalized MD for $\tau_f = [0.4\ 4]$ with $T_\alpha/T = 5$ and 10, respectively. These figures imply that the miss distance of the OGL is less than that of PN for the

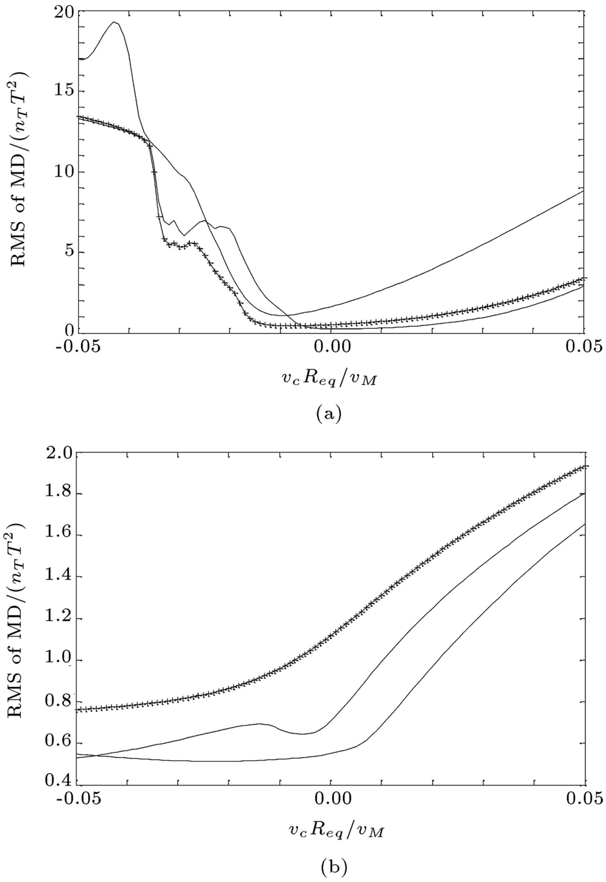

Figure 9. RMS of normalized MD for different intervals of t_f/T with $T_\alpha/T = 10$ and $R_{\text{sat}} = 3$: a) $t_f/T = [0.4\ 20]$; and b) $t_f/T = [0.4\ 4]$.

end game. Also, the preliminary study shows that the proposed modifications to the OGL improve the miss distance of the OGL. For the larger values of τ_f the results are case dependent, but mostly the miss distance of PN is better than OGL, whereas the modified first-order guidance produces less miss distance for the shown intervals when $R_{eq} > 0$. The modified first-order guidance can be utilized when a good approximation of radome slope is available. Better results can be achieved with the adjustment of k_c.

It should be noted that for the numerical results to be independent of the values of radome slope, Eq. (48) has been simplified by replacement of $N'(1+R)$ with N', which slightly changes the values of navigation ratio. For example, in case of $R = \pm 0.03$ we have $N'(1+R) = N'(1 \pm 0.03)$ which can be negligible at the first stage of the preliminary design.

As mentioned earlier, the preliminary study suggests some modifications to the first-order optimal guidance law. Further modifications should be done in the presence of seeker noises, actuator saturation, fin rate saturation and other unmodeled dynamics in a nonlinear six-degree-of-freedom flight simulation.

7. Conclusions

In this paper, normalized miss distance analysis of single-lag OGL is carried out for the fifth-order binomial guidance and control system with the radome refraction error, acceleration limit, and constant target acceleration. The body rate feedback is also added to the OGL as a well-known classical compensation method for radome effect. Moreover, the stability criteria are obtained for the first- to fifth-order guidance and control system. It is seen that the stability criteria for the first- to third-order guidance and control system impose no upper bound on the two related normalized parameters, whereas they impose some upper bounds on these parameters for the fourth- and fifth-order binomial guidance and control system. The acceleration feedback gain decreases the effective navigation ratio and the equivalent time constant of the guidance and control system. The normalized miss distance curves are useful tools for guidance designer for analysis and design of guidance parameters for an allowable miss distance and acceleration limit. For convenience, the Root Mean Square (RMS) of the normalized miss distance over a specified normalized flight time is utilized to obtain the RMS of normalized MD versus equivalent radome slope (multiplied by closing velocity-to-interceptor velocity ratio). Based on the presented analysis, some modifications to OGL are presented for the end game, which are useful for the design of an end game guidance scheme in a real engagement.

References

1. Garnell, P., *Guided Weapon Control System,* Pergamon Press, 2nd Ed. (1980).
2. Lin, C.-F., *Modern Navigation, Guidance, and Control Processing*, Prentice-Hall, Englewood Cliffs, NJ (1991).
3. Neslin, F.W. and Zarchan, P. "Wing size vs radome compensation in aerodynamically controlled radar homing missiles", *AIAA Journal of Guidance, Control, and Dynamics*, **9**(6), pp. 645-649 (1986).
4. Kozakoff, D.J., *Analysis of Radome-Enclosed Antennas*, 2nd Ed, Artech House, Inc., Norwood, MA (2010).
5. Zarchan, P. *Tactical and Strategic Missile Guidance*, 3rd Ed., AIAA Progress in Astronautics and Aeronautics, **176**, AIAA, Inc., Reston, VA (1997).
6. Neslin, F.W. and Zarchan, P. "Missile guidance design tradeoffs for high altitude air defense", *AIAA Journal of Guidance, Control, and Dynamics*, **6**(3), pp. 207-212 (1983).
7. Neslin, F.W. and Zarchan, P. "Radome induced miss distance in aerodynamically controlled homing missiles", *AIAA Guidance and Control Conference*, AIAA-84-1845, USA (1984).

8. Neslin, F.W. "Missile guidance for low-altitude air defense", *AIAA Journal of Guidance and Control*, **2**(4), pp. 283-289 (1979).

9. Miwa, S. "Radome effect on the miss distance of a radar homing missile", *Electronics and Communications in Japan, Part 1*, **81**(7), pp. 14-22 (1998).

10. Lin, J.-M. and Lin, C.-H. "High altitude air defense with intelligent fuzzy terminal guidance law by taking turning rate and radome error slope into consideration", *Proc. of the 8th Asian Control Conference*, Taiwan, pp. 160-164 (2011).

11. Jalali-Naini, S.H. "Miss distance analysis of proportional navigation using normalized equations with radome effect, saturation, and body rate feedback", *Journal of Aeronautical Engineering*, **14**(1), pp. 1-11 (2012).

12. Cottrell, R.G. "Optimal intercept guidance for short-range tactical missiles", *AIAA Journal*, **9**(7), pp. 1414, 1415 (1971).

13. Neslin, F.W. and Zarchan, P. "A new look at classical versus modern homing missile guidance", *AIAA Journal of Guidance and Control*, **4**(1), pp. 78-85 (1981).

14. Holder, E.J. and Sylvester, V.B. "An analysis of modern versus classical homing guidance", *IEEE Transactions on AES*, **26**(3), pp. 599-605 (1990).

15. Rusnak, I. and Meir, L. "Modern guidance law for high-order autopilot", *AIAA Journal of Guidance, Control, and Dynamics*, **14**(5), pp. 1056-1058 (1991).

16. Ohlmeyer, E.J. and Phillips, C.A. "Generalized vector explicit guidance", *AIAA Journal of Guidance, Control, and Dynamics*, **29**(2), pp. 261-268 (2006).

17. Jalali-Naini, S.H. "Modern explicit guidance law for high-order dynamics", *AIAA Journal of Guidance, Control, and Dynamics*, **27**(5), pp. 918-922 (2004).

18. Evers, J.H., Cloutier, J.R., Lin, C.F., Yueh, W.R. and Wang, Q. "Application of integrated guidance and control schemes to a precision guided missile", *American Control Conference*, Chicago, IL, pp. 3225-3230 (1992).

19. Yanushevsky, R., *Modern Missile Guidance*, CRC Press, Taylor & Francis Group, Boca Raton, FL (2008).

20. Mohammadkhani, M.A. and Nikoosokhan, M. "Stability analysis of homing loop with parasitic feedback", *The 9th Iranian Aerospace Society Conference*, Tehran, Iran (2010).

21. Lin, J.-M. and Chau, Y.-F. "Radome slope compensation using multiple-model Kalman filters", *AIAA Journal of Guidance, Control, and Dynamics*, **18**(3), pp. 637-640 (1995).

22. Han, S.S., Jang, S.K. and Lee, S.J. "Radome compensation using adaptive particle filter", *The 17th IFAC Symposium on Automatic Control in Aerospace*, ICT, Univesitas Stadii Tolosana, France, **17**, Part 1, pp. 43-48 (2007).

23. Lin, C.L. "Stability analysis of radome error and calibration using neural network", *IEEE Transactions on AES*, **37**(4), pp. 1442-1450 (2001).

24. Song, T.L. and Shin, S.J. "Active homing performance enhancement with multiple model radome slope estimation", *AIAA Guidance, Navigation, and Control Conference*, AIAA-2004-4899, Rhode Island, USA (2004).

25. Gurfil, P. and Kasdin, J. "Improving missile guidance performance by in-flight two-step nonlinear estimation of radome aberration", *IEEE Transactions on Control System Technology*, **12**(4), pp. 532-541 (2004).

26. Cao, X., Dong, C., Wang, Q. and Chen, Y. "Radome slope estimation in flight using fuzzy adaptive multiple model for active homing missile", *The 9th International Conference on Electronic Measurement & Instruments*, Beijing, China, pp. 1017-1022 (2009).

27. Zarchan, P. and Gratt, H. "Adaptive radome compensation using dither", *AIAA Journal of Guidance, Control, and Dynamics*, **22**(1), pp. 51-57 (1999).

28. Willman, W. "Radome compensation using dither", *AIAA-98-4415*, pp. 1363-1373 (1998).

29. Palumbo, N.F., Blauwkamp, R.A. and Lioyd, J.M. "Principles of homing guidance", *John Hopkins APL Technical Digest*, **29**(1), pp. 25-41 (2010).

Biography

Seyed Hamid Jalali-Naini received his BS in Mechanical Engineering from Amirkabir University of Technology in 1994 and his MS degree from University of Tehran in 1996 also in Mechanical Engineering. Then he started working as a Research Engineer at Aerospace Research Institute (ARI). In 2004, he entered the PhD program of Aerospace Engineering at Sharif University of Technology and earned his degree in 2008. He is currently an Assistant Professor of Aerospace Engineering at Tarbiat Modares University, Iran. His research interests are in the area of guidance and control of aerospace vehicles.